LASER-ULTRASONIC OPTICAL CHARACTERIZATION OF NONMETALS

A. Hammoutene, F.Enguehard and L.Bertrand

Department of Engineering Physics
École Polytechnique de Montréal
C.P 6079, Succ.Centre-ville
Montréal, Quebec, Canada, H3C 3A7

INTRODUCTION

There is now a growing interest in the use of laser-generated ultrasound for nondestructive evaluation of materials [1,2]. In the case of nonmetals, the laser-ultrasonic displacement signals result from temporal convolution between the optical penetration, the laser pulse duration and the laser spot extension [3,4]. The temporal information present in the first longitudinal arrival called "the precursor" depends on this three parameters [4,5]. A temporal broadening of the precursor with increasing the optical penetration have been already observed experimentally [6]. It has been shown that a measurement of the full width at half maximum (FWHM) of the precursor allows an evaluation of the optical absorption coefficient of the material at the excitation wavelength [7]. To evaluate this coefficient with a good reliability one needs to take into consideration the two other parameter effects (the extension spot size effect and the pulse duration effect). In this paper, first we present experimental and theoretical studies of the optical penetration on the acoustic waveforms. As the laser wavelength was fixed (1064 nm), we have used Schott glasses with identical thermomecanic properties and different optical absorption coefficients. Characteristic curves (in the 1-d and the 2-d regimes) that relates the FWHM of the precursor to the optical absorption coefficient have been plotted. Llinear variation regions have been identified on these curves. We have shown that it is possible to deduce the optical absorption coefficient in these regions by fitting the curves. Optical absorption coefficients of the Schott glasses have been deduced using this approach. Results were in good agreement with data given by the manufacturer and data calculated using a theoretical approach [5].

EXPERIMENT

Samples

The samples used in this work are the following Schott glasses: BG 18, NG 9, NG 4 and NG 11. These glasses have identical thermal and mechanical properties and different optical absorption coefficients. Their optical penetration depths are sufficient to generate clearly observed precursors. The physical properties of our samples are summarized in Table 1.

Review of Progress in Quantitative Nondestructive Evaluation, Vol. 17
Edited by D.O. Thompson and D.E. Chimenti,, Plenum Press, New York, 1998

Table 1. Physical Properties of the Schott Glass Samples

Schott glass sample	Density	Specific heat C_v (J/kg°K)	optical penetration depth (μm) at 1064 nm	Thermal expansion Coefficient α (°K^{-1})	Poisson ratio
BG-18	2680	700	103	8.10^{-6}	0.23
NG-9	2680	700	334	8.10^{-6}	0.24
NG-4	2680	700	808	8.10^{-6}	0.25
NG-11	2680	700	1900	8.10^{-6}	0.24

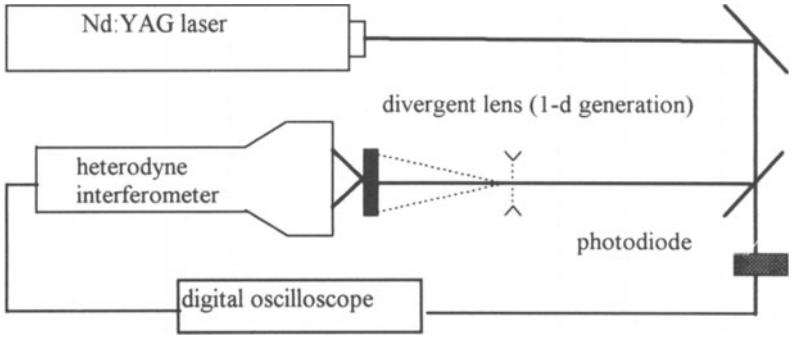

Figure 1. Experimental setup.

Experimental Setup

An experimental setup that uses an optical heterodyne interferometer to detect laser ultrasound has already been described [8]. The laser generation was a monomode pulsed Nd-YAG with a gaussian radius of 1.5 mm and a pulse duration of 20 ns. In this configuration, the spot size was sufficiently small to generate both longitudinal and transverse acoustic waves (2-d generation). In this paper, we have used a second configuration where a divergent lens have been insert at 30 cm far from the sample to obtain a diameter of the excitation beam sufficiently large to generate only longitudinal acoustic waves (Figure 1).

Experimental Results

The 1-d and the 2-d experimental displacement curves are respectively represented in Figure 2 and Figure 3. In most of the figures shown below, the noise observed at the beginning of the curve arises from electromagnetic interference from the laser. In the 1-d regime, we observe the precursor and its multiple reflections at the free boundaries of the plate. In the 2-d regime, both longitudinal and transverse displacements are observed. This last one is identified by the shear wave arrival situated between the first two precursors. This wave is mode-converted into a longitudinal wave at the first-encountered free boundary and then repeated with the longitudinal arriving time. Concerning the precursor features, the increase of the optical penetration induce a temporal broadening attended with a decrease of its amplitude both in the 1-d and 2-d regimes. This can be explained by the fact that thermoelastic sources are activated over the whole region where the light has penetrated into the material. These buried thermoelastic sources induce normal displacements more and more intense (according to the Beer-Lamber loi: more the light penetrates into the material, less is the intensity of the thermoelastic source) until the arrival of the negative displacement originating from the front side of the sample impinged at t=0. In the particular case of a nearly transparent material, one can notice that thermoelastic sources are activated on the rear side of the sample and generate normal displacement at t=0 [4].

THEORY: Thermoelastic Generation of Ultrasound in Nonmetals

Basic Brincipals

In the thermoelastic regime, the absorption of a laser pulse by a sample induces a localized thermal expansion which in turn generates ultrasonic waves. In the case of nonmeltals, the temperature elevation field is assumed to be dictated by the optical absorption only. This field is given by the heat diffusion equation:

$$\rho C_p \frac{\partial T}{\partial t} = \nabla.([k].\nabla T) + \beta I_0 g(x,y) f(t) \qquad (1)$$

where ρ is the density, C_P the specific heat, [k] the thermal conductivity tensor, β is the optical absorption coefficient, I_0 the energy absorbed by the sample. g(x,y) and f(t) represent respectively the normalized surface and time distributions of the laser radiation. The mechanical displacement fields in the case of an orthotropic plate are dictated in the

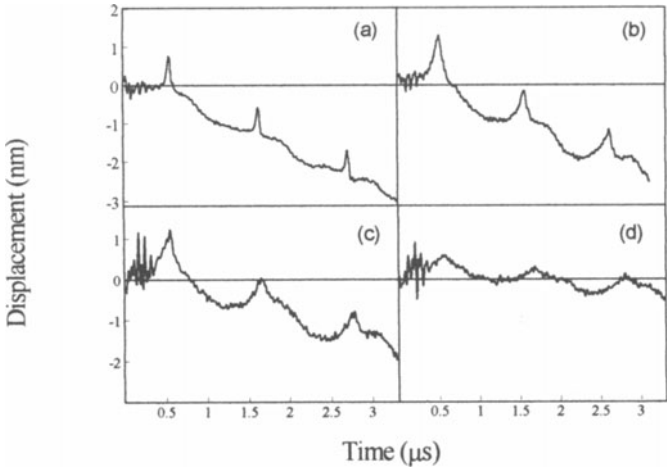

Figure 2. 1-d experimental displacement curves : (a) BG18 Schott glass, (b) NG9 Shott glass , (c) NG4 Schott glass, (d) NG11Schott glass.

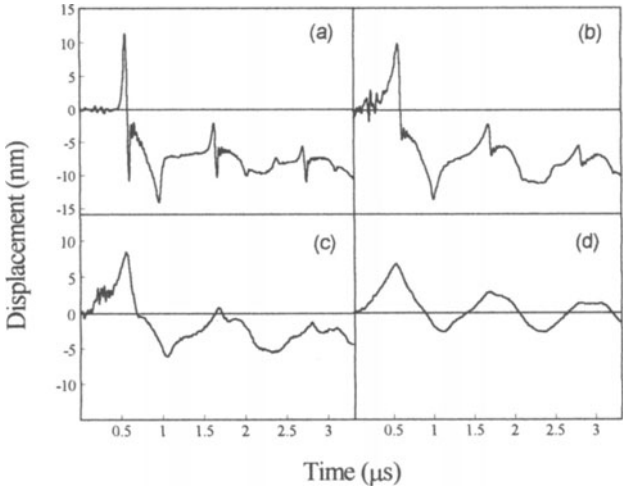

Figure 3. 2-d experimental displacement curves : (a) BG18 Schott glass, (b) NG9 Shott glass , (c) NG4 Schott glass, (d) NG11Schott glass.

cylindrical coordinates system by the following wave equations:

$$\begin{cases} \rho\dfrac{\partial^2 u_r}{\partial t^2} = C_{11}\left(\dfrac{\partial^2 u_r}{\partial r^2}+\dfrac{1}{r}\dfrac{\partial u_r}{\partial r}-\dfrac{u_r}{r^2}\right)+C_{44}\dfrac{\partial^2 u_r}{\partial z^2}+\left(C_{13}+C_{44}\right)\dfrac{\partial^2 u_z}{\partial r\partial z}-\lambda_r\dfrac{\partial(\Delta T)}{\partial r} \\ \rho\dfrac{\partial^2 u_z}{\partial t^2} = C_{44}\left(\dfrac{\partial^2 u_z}{\partial r^2}+\dfrac{1}{r}\dfrac{\partial u_z}{\partial r}\right)+C_{33}\dfrac{\partial^2 u_z}{\partial z^2}+\left(C_{13}+C_{44}\right)\left(\dfrac{\partial^2 u_r}{\partial r\partial z}+\dfrac{1}{r}\dfrac{\partial u_r}{\partial z}\right)-\lambda_z\dfrac{\partial(\Delta T)}{\partial z} \end{cases} \quad (2)$$

where, u_r and u_z are respectively the displacement fields in the radial plan and in the direction of the thickness, C_{11}, C_{44}, C_{13}, and C_{33} the elastic constants of the material and λ_r and λ_z the stiffness -expansion constants [9].
The resolution of this set of equations can be made by using the temporal Laplace and the spatial Hankel transformations. By performing numerical inverse Laplace and Hankel transformations of the solution, we finally obtain the displacement field as a function of time and space. Using this resolution method, we have developed a 2-d model [10] that allows to take into consideration all the parameters involved in a laser ultrasonic experiment (the source and sample features). The parameter of interest in this paper is the optical absorption coefficient. It is represented by a dimensionless number βd. d is the sample thickness.

Quantitative Analysis and Determination of β

In this paper, we are interested in the FWHM of the precursor. With the help of the 2-d model described below we have simulated ultrasonic displacements corresponding to our experimental conditions for a large range of the parameter (βd). We have then plotted the variations of the FWHM of the precursor as a function of the optical penetration depth in the 1-d and 2-d regimes as shown in Figure 4 and Figure 5.
We have identified linear variation regions of the FWHM which can be represented through a relation between the FWHM and β as follows:

$$\log\left(\frac{FWHM}{t_l}\right) = a.\log(\beta d) + b \quad (3)$$

where a and b are two parameter related to the linearity of the curve in the region of interest. We can write equation (3) in the following way:

$$\frac{FWHM}{t_l} = (\beta d)^a e^b \quad (4)$$

Where, FWHM and t_l are measured from the experimental precursors, the thickness d is measured using a micrometer and the parameters a and b are determined numerically using a linear regression. Finally, the measurement of the FWHM, t_l and d and the knowledge of a and b will allow us to determine β through equation (4).
Results concerning the 1-d and 2-d regimes are reported in the tables 2 an 3. They are compared with data given by the manufacturer with good agreement. In the 1-d regime results are also compared to data obtain theoretically using the approach proposed by Dubois et al [5]. In the case of the NG-9 glass sample, our value of β is in good agreement with the one caculated theoretically but in disagreement with the value given by the manufacturer. This is probably due to a mistake in the edition of the catalogue given by the manufacturer.

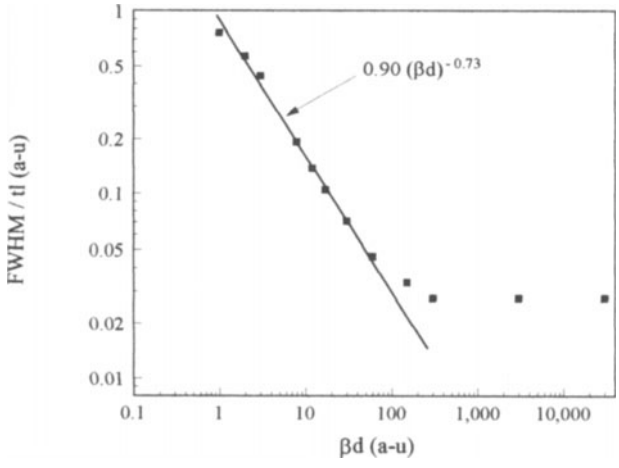

Figure 4. FWHM as a function of the optication absorption coefficient in the 1-d regime, showing the linear area obtained by linear regression.

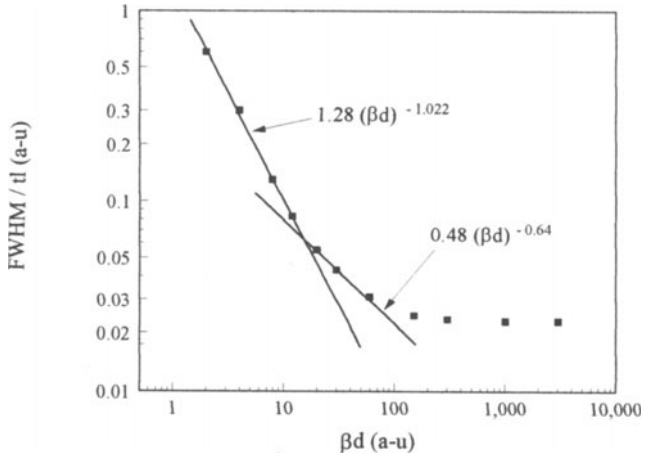

Figure 5. FWHM as a function of the optication absorption coefficient in the 2-d regime, showing the linear areas obtained by linear regression.

Otherwise, the BG-18 value of β determined in the 2-d regime is erroneous. We thought that this is related to the fact that we have reached the bandwidth limit of our interferometric detection system.

Table 2. Summary of the measurement results of β in the 1-d configuration.

Sample	BG-18	NG-9	NG-4	NG-11
Thickness (μm)	3098	3055	3065	3099
1-d configuration				
FWHM (ns)	43	127	170	330
t_l (ns)	544	544	544	555
β (m^{-1}) our approach	9044	2122	1405	562
given by the manufacurer	9259	3333	1238	526
calculated [14]	5664	1973	1459	745

Table 3: Summary of the measurement results of β in the 2-d configuration.

2-d configuration				
FWHM (ns)	40	112	171	373
t_l (ns)	538	546	548	534
β (m^{-1}) our approach	6259	2013	1311	583
given by the manufacurer	9259	3333	1238	526

CONCLUSION

We have presented an approach that allows us to relate the optical absorption coefficient of a nonmetal material to the FWHM of the precursor. Experiments performed on glass samples with different optical coefficients at 1064 nm have demonstrated the possibility to measure a large range values of this coefficient by the laser-ultrasonic technique both in the 1-d and 2-d configurations.

REFERENCES

1. C.B. Scruby, L.E. Drain, *Laser-Ultrasonics: Techniques and applications*, (Adam Hilger, Bristol, UK 1990).
2. J.P.Monchalin and J.D.Aussel, *Journal of nondestructive evaluation*, 9 (4) (1990) 211- 221
3. F.A.McDonald, *Appl. Phys.Lett.*, 56(3),230 (1990).
4. F.Enguehard, L.Bertrand, *J. Appl.Phys,*82(4) (1997) 1532-1538.
5. M.Dubois, F.Enguehard and L.Bertrand, *Phys.Rev. E,*50 (2) (1994) 1548-1551.
6. G.C.Wetsel, *IEEE Transaction on Ultrasonics, Ferroelectrics, and frequency control,*UFFC-33 (5) (1986)450-461.
7. M.Dubois, F.Enguehard, L.Bertrand, M. Choquet and J.P. Monchalin, *J. de Phys.*4 (1994)C7-689-C7 692.
8. A.Hammoutene, F.Enguehard, L.Bertrand, *Review of Progress in QNDE , Vol.*16 Ed. By D.O. Thompson and D.E. Chimenti, (Plenum Press, NY,1997) 483-490.
9. M.Dubois, F.Enguehard and L.Bertrand, *Appl. Phys.Lett.*, 64 (5),554-556 (1994)
10. E.Lafond, F. Enguehard, A. Cournoyer, J-P Longuemard, to be published in the proceedings of the *World Congress on Ultrasonics Conference*. (Berlin,Sept 1995).